DEVELOPMENT AND GEOMETRIC VALIDATION OF ALUMINUM VACUUM CHAMBER PROTOTYPES FOR THE SPS-II STORAGE RING*

T. Phimsen[1,†], S. Boonsuya[1], S. Chitthaisong[1], W. Woranut[1], K. Trongklang[1], A. Kwankasem[1], S. Sumklang[1], O. Seegauncha[1], J. Sukain[1],
[1] Synchrotron Light Research Institute, Nakhon Ratchasima, Thailand

Abstract

This paper details the manufacturing and geometric validation of two aluminum alloy vacuum chamber prototypes for the 3.0 GeV Siam Photon Source II (SPS-II) storage ring: a straight-section chamber and a bending chamber. Key technological advancements include the optimization of domestic aluminum extrusion processes

Key technological advancements include the optimization of domestic aluminum extrusion processes to achieve ultra-high vacuum (UHV) surface requirements and the implementation of oil-less, ethanol-cooled CNC machining to eliminate hydrocarbon contamination while maintaining high precision. A comprehensive metrology framework, utilizing laser trackers and high-resolution profiling, was employed to characterize manufacturing-induced distortions. Results confirm that the integrated fabrication workflow, which combines specialized internal fixturing and multi-pass TIG welding, successfully maintains the stringent geometric tolerances required for the storage ring. This work validates the technical readiness of Thailand's industrial sector for the full-scale production of the SPS-II vacuum system.

INTRODUCTION

The Siam Photon Source II (SPS-II) is a 3.0 GeV fourth-generation light source utilizing a Double Triple Bend Achromat (DTBA) lattice [1, 2]. The ultra-low natural emittance design requires high-gradient magnets with small bore radii, reducing the clearance between the vacuum chamber exterior and magnet poles to the sub-millimeter level [2].

Concentrating high-capacity pumping near the photon absorbers yields a simulated average pressure of 1.1×10^{-9} mbar after 100 Ah of beam conditioning [2, 3]. The vacuum chambers are fabricated from aluminum alloys, A6061-T6 for arc section bending chambers and A6063-T5 for straight section extrusion profiles, selected for their favorable combination of low outgassing rate, high thermal conductivity, and machinability [2, 3].

DESIGN SPECIFICATIONS AND ACCEPTANCE CRITERIA

The prototyping program addresses a middle straight chamber and a VCB-4 bending chamber. Table 1 summarizes the specific geometric tolerance criteria and vacuum integrity requirements derived from lattice aperture constraints.

Table 1: Prototype Deformation Acceptance Criteria

Parameter	Specification
Transverse deformation	< 0.3 mm/m
Longitudinal deformation	< 1.0 mm/m
Deformation Magnet position	< 0.5 mm

STRAIGHT CHAMBER FABRICATION AND VALIDATION

The final dummy chamber design, shown in Fig. 1, adopts a circular main body profile (62.71 mm ID) with integrated cooling channels. This geometry achieved an as-extruded internal surface roughness of R_a 0.162–0.529 µm without requiring additional polishing, confirming that the domestic manufacturer had successfully internalized prior process improvements. To prevent UHV contamination, components underwent standard multi-stage chemical cleaning (alkaline etching, acid passivation, and ultrasonic cleaning) prior to assembly. Welding was performed using a second-generation optimized fixture, developed through the iterative prototyping program [4], in a five-stage sequence designed to minimize accumulated thermal distortion: starting with taper-to-flange sub-assemblies and concluding with the final taper-end attachment. The nominal wall thickness at all welding joints for both the straight extrusion and the VCB-4 bending chamber is maintained at 4 mm. For the VCB-4 chamber, specialized grooves were machined adjacent to the thicker sections and pumping ports to prevent localized heat dissipation, successfully concentrating the thermal input directly at the weld seam. A dual-shielding argon gas system was strictly maintained to protect both the weld pool and the internal bore surface from atmospheric oxidation, ensuring that the internal surface finish remained within UHV specifications.

Following welding, dimensional inspection was conducted using a precision height gauge and digital calipers. The resulting vertical and horizontal deformation profiles are illustrated in Fig. 2. The vertical deformation rate of 0.24 mm/m and horizontal rate of 0.28 mm/m both satisfied the 0.3 mm/m specification. The mean longitudinal length measured was 1531.88 mm, well within the ±1 mm budget. All geometric and integrity results for this prototype are consolidated in Table 2.

† thanapong@slri.or.th

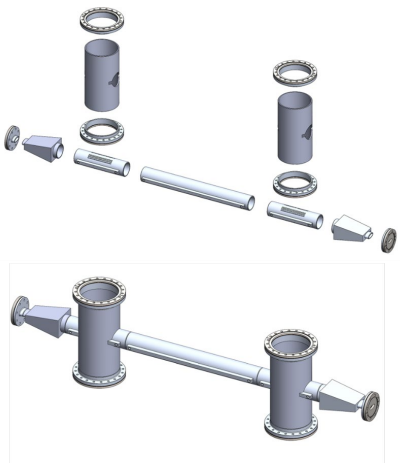

Figure 1: Exploded view of the middle straight dummy chamber assembly showing all major components.

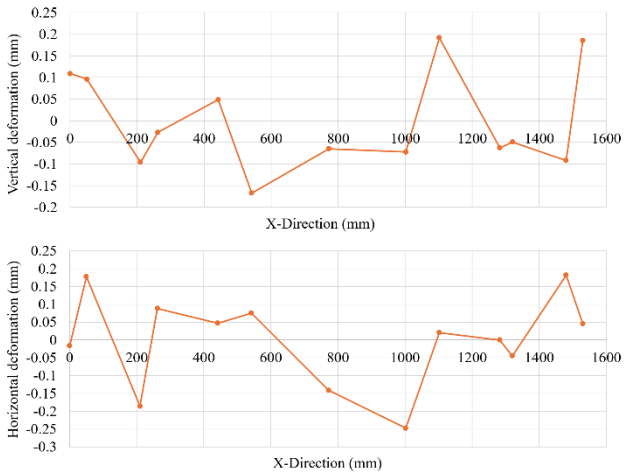

Figure 2: Measured vertical (top) and horizontal (bottom) deformation profiles along the dummy chamber longitudinal axis.

Table 2: Geometric Validation Results For The Middle Straight Dummy Chamber

Deformation	Specification	Measured
Vertical (mm/m)	< 0.3	0.24
Horizontal (mm/m)	< 0.3	0.28
Longitudinal (mm)	< 1.0	0.88
Flange parallelism (mrad)	-	2.45

BENDING CHAMBER FABRICATION AND VALIDATION

The VCB-4 bending chamber represents the most significant manufacturing challenge in the arc section due to its complex three-dimensional curved trajectory. Unlike the straight-section chambers, the VCB-4 must be fabricated from solid A6061-T6 aluminum billets using five-axis CNC machining, as extrusion is not technically feasible for its intricate internal profile. To eliminate hydrocarbon contamination at the source and avoid extensive post-machining remediation, all primary CNC operations were conducted using pure ethanol as the sole cutting fluid. This methodology, adapted from practices developed at the National Synchrotron Radiation Research Center (NSRRC) in Taiwan [5], was performed in a dedicated temporary cleanroom facility.

A custom ethanol spray cooling system, as illustrated in Fig. 3, was integrated with the five-axis machine to deliver the coolant through high-pressure nozzles equipped with inline filtration to prevent oil ingress. The measured dew point in the ethanol stream was recorded at –120°C, which significantly exceeds the –80°C requirement and confirms a machining environment free of both hydrocarbon and moisture contamination. Post-machining inspection confirmed an internal beam duct surface roughness of R_a 0.08 µm, satisfying UHV cleanliness requirements and providing optimal conditions for subsequent TIG welding.

Figure 3: Ethanol spray cooling system installed at N.K.R. Engineering Company for oil-free five-axis CNC machining of the VCB-4 chamber halves.

Following standardized chemical cleaning, the VCB-4 components were assembled via an eight-stage TIG welding sequence. A critical process feature employed for this prototype was the use of pre-heating; heating elements were installed on the external surfaces to raise the structure to 80°C before seam welding commenced. This pre-heat phase is essential to reduce thermal gradients, slow the post-weld cooling rate, and suppress the accumulation of residual stresses, which is of particular importance for the large-aspect-ratio curved geometry of the VCB-4. Longitudinal seam welding was performed in segments with pauses for temperature equilibration. The final helium leak rate was measured at 6.5×10^{-11} mbar·L/s confirming the success of the welding operations.

Geometric characterization of the completed chamber was conducted using two complementary measurement systems: a Leica Absolute Tracker laser interferometer for 3D global coordinates at eight precision fiducial holes and a precision height gauge for a 28-point high-density vertical survey. Singular Value Decomposition (SVD) and the Kabsch algorithm were used to calculate rigid-body alignment and isolate residual manufacturing deviations against design coordinates.

The laser tracker results, after Kabsch alignment, show that the vertical component dominates the deformation field, with the Outside Dipole section exhibiting systematic upward residuals. This behavior is visualized in the 2D deformation heatmap shown in Fig. 4. The high-density height gauge survey corroborated these findings and additionally resolved a torsional deformation mode, a transverse gradient of 0.240 mm, arising from asymmetric thermal stress relaxation during welding. This complex deformation is visualized in Fig. 5.

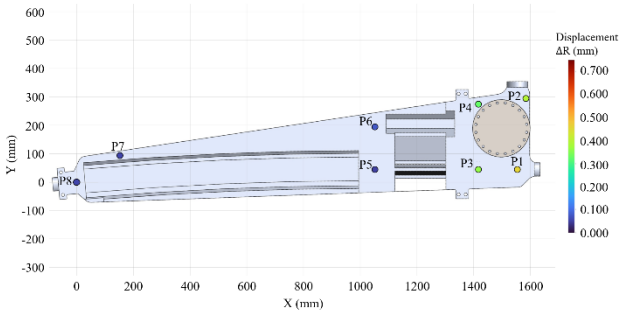

Figure 4: Vertical deformation heatmap from laser tracker

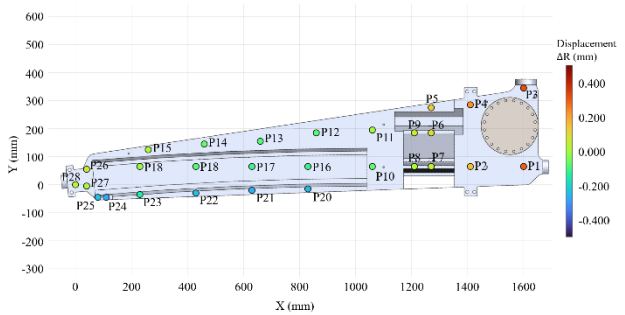

Figure 5: Vertical deformation heatmap from Height gauge measurement

Despite these systematic modes, all measurements confirmed compliance with the ±0.255 mm bilateral tolerance envelope across all axes. Clearance verification at 23 magnetic interface positions yielded vertical deformations ranging from –0.101 mm to +0.092 mm. Against the minimum design radial clearance of 0.5 mm, the maximum observed deformation retains a safety factor exceeding 4:1, ensuring that the structural behavior does not compromise installation or operational safety. It should be noted that these prototype metrology measurements were conducted under ambient pressure with the chambers positioned on precision blocks over a granite table, as the final girder support structures were still undergoing machining. Comprehensive deformation measurements under full vacuum load are planned for the next phase of testing. These results validate the oil-free machining and pre-heated welding workflow as a production-ready methodology for UHV bending chambers.

DISCUSSION

The experimental data reveals that deformation mechanisms differ fundamentally between the two chamber architectures. In straight-section chambers, deviations arise primarily from accumulated dimensional variations at machined mating surfaces, suggesting that tighter CNC toleranceing for interface geometries is the most direct path to increasing the current 7% horizontal deformation margin. Conversely, VCB-4 bending chamber deformation is dominated by the release of residual machining stresses during the welding thermal cycle, producing the characteristic inter-sectional bowing and torsional twist observed in the metrology data. For tunnel installation, a passive tolerance stack-up budget safeguards the magnet clearance envelope. Magnets are adjusted directly on the girders within a combined 20-30 μm tolerance. The chamber is placed unadjusted, relying on a rigid tolerance loop where the girder (20 μm), support (30 μm), and mounting ears (50 μm) guarantee compliance with the relaxed 100 μm chamber positioning requirement.

Furthermore, the thermal activation strategy differentiates between the two architectures; straight sections are specified for an in-situ bakeout at 150°C for 24 hours using integrated bellows, whereas the VCB-4 bending chambers will undergo an ex-situ laboratory bakeout at 150°C for 24 hours prior to installation. Evaluating whether these respective thermal cycles induce further geometric warping via residual stress relaxation represents a vital next step for our engineering team. The dual-modality metrology approach, combining global laser tracker registration with high-density height gauge profiling, was essential for validating the VCB-4. The 31 μm agreement between these two independent datasets provides high confidence in the compliance assessment. Furthermore, the successful implementation of the oil-free ethanol machining process, which achieved a coolant dew point of –120°C, confirms that Thailand's domestic sector can now produce UHV-ready components without the hydrocarbon contamination risks associated with traditional oil-cooled machining.

CONCLUSION

The fabrication and validation of these two prototypes demonstrate that the technical capability for full-scale SPS-II vacuum production has been successfully established within Thailand’s domestic industrial sector. Both the middle straight dummy chamber and the VCB-4 bending chamber achieved full compliance with the acceptance criteria derived from the DTBA lattice magnet aperture constraints. Specifically, the transverse deformations were maintained within the 0.3 mm/m limit, and helium leak rates remained significantly below the threshold. With the manufacturing workflow qualified, straight-section chamber production is authorized to proceed immediately. Bending chamber production will follow, focusing on optimized CNC tool paths to minimize subsurface stress, inter-stage thermal resting (rough, medium, fine), and post-machining stress relief. These results provide the technical foundation required for successful assembly and operation of the SPS-II storage ring.

REFERENCES

[1] P. Sudmuang et al., “SPS-II project: Status update”, in Proc. IPAC'25, Taipei, Taiwan, Jun. 2025, pp. 903-908. doi:10.18429/JACoW-IPAC2025-TUZD2

[2] T. Phimsen *et al.*, “Vacuum system design and simulation for Siam Photon Source II: Towards Thailand's fourth-generation synchrotron light source”, in *Vacuum,* vol. 240, p. 114569, 2025.doi:10.1016/j.vacuum.2025.114569.

[3] T. Phimsen *et al.*, “Progress in vacuum system design for Thailand's new light source”, in *Vacuum,* vol. 234, p. 114111, 2025.doi: 10.1016/j.vacuum.2025.114111

[4] T. Phimsen *et al.*, “Fabrication challenges and lessons learned in prototyping SPS-II straight section vacuum chambers”, in *Proc. 13th Int. Conf. Mech. Eng. Design Synchrotron Radiat. Equip. Instrum. (MEDSI'25)*, Lund, Sweden. doi:10.18429/JACoW-MEDSI2025-WEP22

[5] G.-Y. Hsiung et al., “TPS vacuum system”, in Proc. PAC'09, Vancouver, Canada, May 2009, paper MO6RFP018, pp. 387-389.